



Draft Muon Collider Parameters Version 1.1  
R. B. Palmer  
Brookhaven National Laboratory  
12/14/2011

## Contents

<b>1</b>	<b>Introduction to this study</b>	<b>2</b>
<b>2</b>	<b>Assumptions</b>	<b>3</b>
2.1	Cryostat losses at 4 K . . . . .	3
2.2	Room temperature cavity parameters . . . . .	4
2.3	Superconducting rf . . . . .	4
2.4	Induction acceleration . . . . .	5
2.5	RLA Droplet Arc lengths vs E . . . . .	5
<b>3</b>	<b>Sub-systems</b>	<b>6</b>
3.1	Proton driver . . . . .	6
3.2	Target, Capture and Taper . . . . .	6
3.3	Phase Rotation . . . . .	7
3.3.1	Introduction . . . . .	7
3.3.2	Neutrino Factory Phase Rotation to 21 bunches . . . . .	8
3.3.3	Muon Collider Phase Rotation to 12 bunches . . . . .	8
3.4	Charge Separation . . . . .	9
3.4.1	Neutrino Factory Charge Separation . . . . .	9
3.4.2	Muon Collider Charge Separation . . . . .	9
3.5	6D cooling . . . . .	10
3.5.1	Introduction . . . . .	10
3.5.2	Neutrino Factory: Transverse 4D Cooling . . . . .	11
3.5.3	Guggenheim Cooling . . . . .	11
3.5.4	Helical Cooling Channel (HCC) . . . . .	14
3.6	Bunch Merging . . . . .	16
3.6.1	Muon Collider 6D Merge of 21 bunches . . . . .	16
3.7	Muon Collider Final 4D Cooling . . . . .	17
3.7.1	Introduction . . . . .	17
3.7.2	rf parameters of stages . . . . .	17
3.7.3	Room Temperature Acceleration from 6 to 400 MeV . . . . .	18
3.8	Super-Conducting Acceleration . . . . .	19
3.8.1	Neutrino Factory Acceleration with FFAG . . . . .	19
3.8.2	Muon Collider Acceleration with FFAG . . . . .	19
3.8.3	Acceleration with improved transmission . . . . .	21
3.9	Collider Ring for 1.5 TeV c of m . . . . .	22
3.9.1	Ring Magnet Shielding of Decay Electrons . . . . .	23
<b>4</b>	<b>Summaries</b>	<b>24</b>
4.1	Introduction . . . . .	24
4.2	Production and transmission . . . . .	24
4.3	Wall Power . . . . .	25
4.3.1	Baseline at 1.5 TeV c of m . . . . .	25
4.3.2	At 3 TeV instead of 1.5 TeV c of m . . . . .	25
<b>5</b>	<b>Conclusion</b>	<b>26</b>

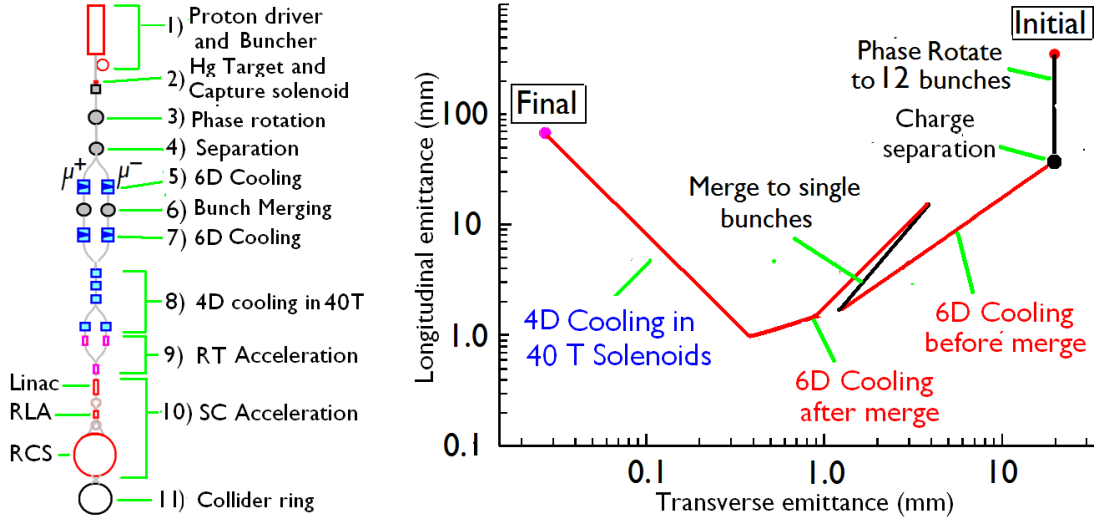


Figure 1: a) Schematic of a Muon Collider; b) Approximate trace of longitudinal and transverse emittances through stages 3 to 8 of this Muon Collider. The stage numbers will be used in the discussion below.

## 1 Introduction to this study

This is not intended to be a definitive tabulation of accepted Muon Collider parameters. It has been compiled using a variety of sources, and makes assumptions to obtain parameters that are not available or unknown to the authors. Its object is to gain insight into the orders of magnitudes of our proposal, not an actual description. It arose from a request for a list of all the needed rf systems, but it goes a little beyond that, including some magnet specifications, but it is far from complete. Where there are multiple technology options, these will be mentioned and sometimes tabulated, but for the summaries at the end, only one choice of technologies will be used. In some cases, parameters for a Neutrino Factory are also given for comparison.

Figure 1 a shows a schematic of the Muon Collider configuration. Figure 1 b shows the emittances for the numbered stages from before the phase rotation to end of cooling.

For both Neutrino Factory and Muon Collider, we assume 1) a 4 MW 8 GeV proton Driver, although the pulse structures are different. Then there is a pulse compression system followed by 2) a mercury target in a 20 T solenoid to stabilize the jet and capture the pions. The capture is followed by tapered solenoids feeding a decay channel at a lower field. The resulting flux with wide momentum spread but short time is (3) Phase Rotated into a train of bunches with smaller momentum spread but longer time spread. The method uses rf over a range of frequencies ending in 201 MHz.

After the phase rotation, the differences between Muon Collider and Neutrino Factory systems become larger. For the IDS Neutrino Factory [1] there is no (4) charge separation till after ionization cooling and the only (5) cooling takes place in a linear channel with alternating axial solenoids and plane parallel Lithium Hydride absorbers.

For the Muon Collider [2], after the phase rotation, the charges must be separated to allow (5) 6 dimensional (6D) cooling in a Guggenheim [3] or HCC [4] ionization cooling in curved cooling channels. The initial cooling in a FOFO Snake [5], which works for both signs simultaneously, would delay and simplify the charge separation, but this is not considered here.

When the initial 6D cooling has sufficiently lowered the emittances, the best bunches are (6) merged into single bunches: one of each sign. Earlier designs, including the one used here, merge approximately 12-21 bunches. The merging can be done in just the longitudinal (momentum and bunch length) dimensions, but matching back into 6D cooling is more efficient if it is done in all 6 dimensions. The 6D design used for this study, starting with 21 bunches.

These combined bunches are further 6D cooled, followed by (8) Final Transverse Cooling in 40 T

solenoids. The re-acceleration in later stages of this Final Cooling, use room temperature rf, and finally induction linacs, and may require the charges to be separated.

The acceleration after cooling is initially in (9) room temperature rf with progressively higher frequencies. Eventually, the bunches are short enough to be accelerated in (10) super-conducting rf: first in a linac, then in RLAs [6], and finally in (pulsed) Rapid Cycling Synchrotrons (RCSs) [7]. The beams are then injected, in opposite directions, into the (11) collider ring where the bunches intersect at two opposite locations inside two detectors.

There are many known inconsistencies in the designs and parameters given here, and in the simulations used to obtain the performance of those systems. For example:

- The performance of the muon collider 6D cooling used output from the longer Neutrino Factory phase rotation, rather than the proposed shorter phase rotation design whose parameters are given here.
- The bunch merging used, combined 21 ( $3 \times 7 = 21$ ). rather than 12, as would be more appropriate for the shorter bunch train from the shorter phase rotation.
- The charge separation scheme, whose performance was used to estimate overall transmission, operated at a momentum of 400 MeV/c; whereas the phase rotation that proceeds it operates at 212 MeV/c and the 6D cooling that follows it operates at 200 MeV/c. Since charge separation at lower momenta was found to be too inefficient, a modified phase rotation, or acceleration after it, would be required, but has not yet been designed or simulated, and is not included in the sum of wall power consumption.
- The parameters and performance of the final cooling in 40 T solenoids assumes an initial momentum of 135 MeV/c whereas the last 6D cooling section that preceded it used 200 MeV/c. The match between these is not included.
- It has been determined that there are significant space charge problems in both the late stages of 6D cooling (longitudinal) and early stages of final cooling (transverse). Modifications of the parameters appear to be able to avoid these problems, but these modified parameters are not used here.
- The acceleration schemes discussed here are not real designs and have not been simulated. Real designs are being developed, but are not yet included.

Much more work, approaching an end-to-end simulation, will be needed before the parameters and performance can be give with certainty. As stated above, this tabulation is only intended to get orders of magnitudes for the parameters, not define them.

## 2 Assumptions

### 2.1 Cryostat losses at 4 K

- Cryostat losses are estimated as fixed values per meter of cold systems. We use for this the MICE [8] proposal numbers  $3.3 \text{ W/cell} = 1.2 \text{ W/m}$ .
- This value is then doubled to cover transfer losses, giving  $2.4 \text{ W/m}$
- Cryogenic efficiency is taken to be 20 % of the Carnot efficiency [9], giving  $0.2 \times 4/293 = 0.0027$ .
- This gives a wall power of  $0.9 \text{ kW/m}$

## 2.2 Room temperature cavity parameters

1. At 201 MHz

gap $L$	46.6	cm
grad $\mathcal{E}$	15.5	MV/m
Voltage $V$	7.22	MV
Peak Power $P_{peak}$	4.04	MW
Average Power $P_{cw}$	3.1	MW
rf pulse length $t_{rf}$	$3\tau = 160$	$\mu\text{sec}$

2. For  $f \geq 201$  MHz

$$\mathcal{E} = \mathcal{E}(201) \left( \frac{f}{201} \right)^{0.5}$$

$$\frac{P_{peak}}{L} = \frac{P_{peak}}{L}(201) \left( \frac{\mathcal{E}}{\mathcal{E}(201)} \right)^2 \left( \frac{201}{f} \right)^{1/2}$$

$$t_{rf} = t_{rf}(201) \left( \frac{201}{f} \right)^{3/2}$$

3. For  $f < 201$  MHz

$$\mathcal{E} = \mathcal{E}(201) \left( \frac{f}{201} \right)^{1.25}$$

$$P_{peak} = P_{peak}(201) \left( \frac{f}{201} \right)^{-2}$$

$$t_{rf} = t_{rf}(201) \left( \frac{f}{201} \right)^2$$

where  $\mathcal{E}(201)$  and  $P_{peak}(201)$  are the rf gradient and peak power at 201 MHz.

## 2.3 Superconducting rf

1. At 201 MHz

	Linac 1	all others	
Frequency $f$	201	201	MHz
Length per cavity $L$		75	cm
Ave gradient $\mathcal{E}$	15	17	MV/m
Peak power/cavity $P_{peak}$	0.49	0.508	MW
Pulse lengths $t_{rf}$	3	3	ms

2. At other frequencies and gradients we assume:

$$\mathcal{E} = \mathcal{E}(201) \left( \frac{f}{201} \right)^{0.28}$$

For use in linacs or RLAs we scale the pulse lengths and thus peak rf power as though it were a room temperature cavity:

$$t_{rf} = t_{rf}(201) \left( \frac{201}{f} \right)^{3/2}$$

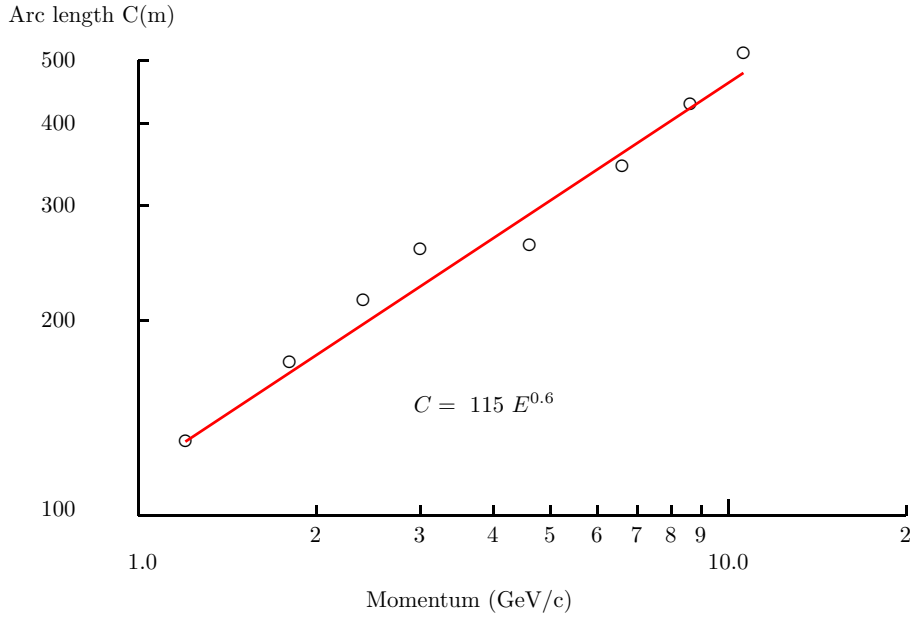


Figure 2: Droplet arc length vs. momentum of muons.

$$P_{peak} = P_{peak}(201) \left( \frac{\mathcal{E}}{\mathcal{E}(201)} \right)^2 \left( \frac{201}{f} \right)^{1/2}$$

For use in an RCS, the peak power is set to match the power removed by the beam and the rf pulse duration is set to the acceleration time plus a shorter initial filling time.

## 2.4 Induction acceleration

We assume performance somewhat less than that used in the Feasibility Study II [10] for a Neutrino Factory. The induction units there were designed by an engineer with real experience in induction accelerators used for other applications.

$$\mathcal{E} \approx 1\text{MV/m} \quad \text{cf Study 2} \quad \mathcal{E} = 1.5\text{MV/m}$$

$$\frac{J}{L} \approx 2.7\text{kJ/m} \quad \text{cf Study 2} \quad \frac{J}{L} \approx 1.9\text{kJ/m}$$

## 2.5 RLA Droplet Arc lengths vs E

Alex Bogacz[6] has designed RLAs for a Neutrino factory with differing arc lengths as a function of the beam momenta. In order to consider designs for a Muon Collider using different momenta, we need a parameterization of the arc lengths vs momentum. This we derive by fitting Alex's different arcs.

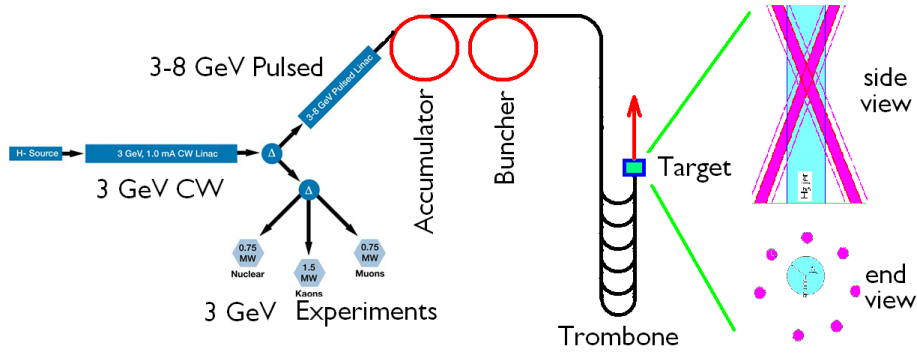


Figure 3: Project X proton driver with modifications as Muon Collider driver.

### 3 Sub-systems

#### 3.1 Proton driver

Specification:

Power	P	4	MW
Repetition rate	f	15	Hz
Proton Energy	$E_p$	8	GeV
Protons per pulse	$N_p$	208	Tp
rms pulse length	$\tau$	2	ns

A task-force [11] led by K. Gollwitzer has studied modifications of the Fermilab proposed Project X for a 3 GeV CW proton linac. The proposed modifications include an upgrade of the CW linac to 5 mA, the addition of a 5 GeV pulsed linac that would take a fraction of the 3 GeV beam and accelerate it to 8 GeV. An accumulator ring at 8 GeV would combine the 6 msec pulses from this linac, forming 4 or more bunches each with approximately  $50 \cdot 10^{12}$  protons. At the end of each accumulation period, these bunches would be transferred to a buncher ring and compressed to rms lengths of 2 nsec. At the required repetition rate of 15 Hz, the bunches would be extracted into four separate (trombone [12]) channels whose lengths would be chosen to bring all four bunches onto the target at the same time. By bringing the four beams onto the liquid metal target from different azimuthal angles, the effective target length can be the same for all bunches.

#### 3.2 Target, Capture and Taper

The target and taper shown in fig. 4, whose parameters given below, is based on the current draft of the Neutrino Factory Initial Design Report (IDR).

A 20 T solenoid over an 8 cm radius aperture will capture all particles from a source on the axis with transverse momenta less than 240 MeV/c which includes the majority of pions which can be captured by the following phase rotation system. The 20 T field is generated by a hollow copper conductor solenoid generating 6 T using 11.5 MW of power. Superconducting solenoids outside the copper coils give the remaining 14 T and provide a tapering field down to that required. Shielding by tungsten carbide beads in water is provided both inside the copper coil, and between it and the superconducting coils.

The energy deposited in SC coils (#1-#19) is [13] 0.86 kW. If the cryogenic efficiency = 20 % of the Carnot efficiency:  $0.2 \times 4/293 = 0.0027$ , then the wall power is  $0.86 \text{ kW}/0.0027 \approx 0.32 \text{ MW}$ .

Resistive coils

Superconducting coils

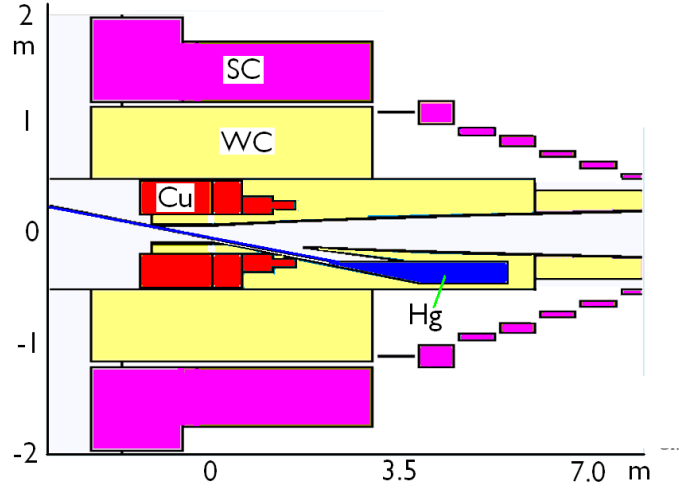


Figure 4: Design of proton target with hybrid Resistive (Cu) and superconducting (SC) 20 T capture solenoid and superconducting taper solenoids. Tungsten Carbide (WC) bead in water shielding is shown in yellow.

	$Z_1$ cm	$\Delta Z$ cm	$R_1$ cm	$\Delta R$ cm	$I/A$ $kA/cm^2$
R 1	-87.7	90.3	18.34	4.76	2.222
R 2	-112.6	143.7	23.8	5.04	1.979
R 3	-120.5	206.8	29.57	5.94	1.428
R 4	-126.1	212.4	36.18	6.44	1.213
R 5a	-129.3	107.8	43.3	6.87	1.068
R 5b	-21.5	107.8	43.3	6.87	1.068

	$Z_1$ cm	$\Delta Z$ cm	$R_1$ cm	$\Delta R$ cm	$I/A$ $kA/cm^2$
SC 1	-243.9	355.9	120	73.28	2.003
SC 2	114	78.4	120	59.84	2.251
SC 3	194.3	100.7	120	18.22	2.813
SC 4	305	65	110	15.3	3.451
SC 5	380	65	100	10.55	3.789
SC 6	455	65	90	7.47	4.069
SC 7	530	60	80	8.58	4.251
SC 8	610	60	55	4.99	4.521
SC 9	680	65	50	4.61	4.603
SC 10	755	65	45	4.14	4.674
SC 11	830	65	45	3.95	4.707
SC 12	905	65	45	3.66	4.732
SC 13	980	65	45	3.43	4.752
SC 14	1055	65	45	3.23	4.768
SC 15	1130	65	45	3.07	4.78
SC 16	1205	65	45	2.96	4.79
SC 17	1280	65	45	2.86	4.798
SC 18	1355	65	45	2.88	4.804
SC 19	1430	140	45	2.68	4.806

### 3.3 Phase Rotation

#### 3.3.1 Introduction

After an initial drift there is a correlation between energy and time. This correlated distribution is now bunched by a sequence of rf cavities whose frequencies, changing with distance, are chosen to keep each forming bunch at the same rf phase. Once bunched, the rf phases are modified to decelerate the early high energy bunches and accelerate the late low energy bunches, leading to a train of bunches at the same mean energy of around 130 MeV.

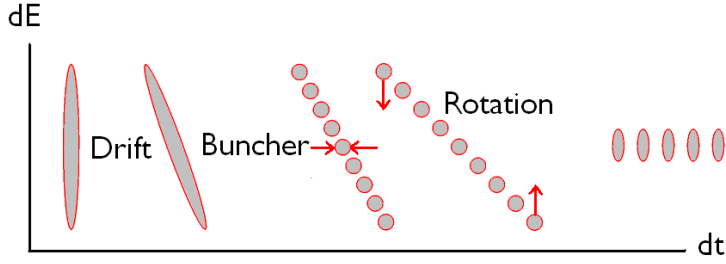


Figure 5: Schematic of phase rotation method. Large  $\Delta E$  small  $\Delta t \rightarrow$  small  $\Delta E$  larger  $\Delta t$ .

### 3.3.2 Neutrino Factory Phase Rotation to 21 bunches

This design [14] generates a relatively long train of bunches, all of which can be used in a Neutrino Factory, but which are harder to merge for a Muon Collider. It is however the design used in the cooling simulations shown later.

In the following table, the rf frequencies  $f$  and rf gradients  $\mathcal{E}$  are given as approximate because they cover significant ranges, the frequencies starting higher than the values given and falling somewhat lower. The approximate values are used in the estimates of power.  $P_{pk}$  is the peak rf power per cavity.  $P_{pktot}$  is  $P_{pk}$  times the number of cavities, except for the buncher where it is half this value reflecting the ramp up of the gradient along the lattice.  $t_{rf}$  is the rf pulse length.  $P_{ave}$  is the average of time of rf power to the cavities.  $P_{wall}$  is the wall power for this rf, assuming a 60% klystron and power supply efficiency.  $N_\mu$  is an average number of muons in this section.

The following, blue parenthesized notes refer to files or programs used to store or derive the data. They are given to help the authors in future upgrades and do not have content for readers.

(from runprmw param4p1)

	E1 MeV	E2 MeV	f MHz	cavs	gap m	Lrf m	L m	$\mathcal{E}$ MV/m	$P_{peak}$ MW	$P_{pktot}$ MW	$t_{rf}$ $\mu s$	$P_{ave}$ MW	$P_{wall}$ MW	$N_\mu$ $10^{12}$
Drift	130.000	130.000	0	0	0.0	0	58	0.0	0.00	0.0	0	0.00	0.00	19
buncher	130.000	130.000	$\approx 300$	44	0.5	22	33	$\approx 8.0$	0.59	13.0	88	0.02	0.03	$21 \times 0.8$
rotation	130.000	130.000	$\approx 210$	56	0.5	28	42	$\approx 12.0$	2.27	127.0	150	0.29	0.48	$21 \times 0.6$
Totals	0.999	130.000		100		50	133			140		0.30	0.50	$21 \times 0.4$

Besides the muons there are significant numbers of other particles that will load the rf, but are not included, but an estimate of power dissipated in the 4 degree coils is made using the data shown in fig. 13 of the IDR (average of G4beamline and ICOOL):

The energy lost as electrons  $\approx 9$  kW, and to protons  $\approx 9$  kW. Not all this will be deposited in the coils and shielding should help, Assuming a reduction of two, the total is  $(9 + 9)/2 = 9$  kW. With a refrigerator efficiency at 20% Carnot of 0.0027, then the wall power used is  $9 / 0.0027 = 3.3$  MW. The Cryostat static losses for 133 m give a wall power requirement of  $133 \times 0.9/1000 = 0.12$  MW.

### 3.3.3 Muon Collider Phase Rotation to 12 bunches

This is a more recent design by Neuffer [15] that is shorter, uses higher gradient rf and delivers approximately the same number of muons in fewer bunches.

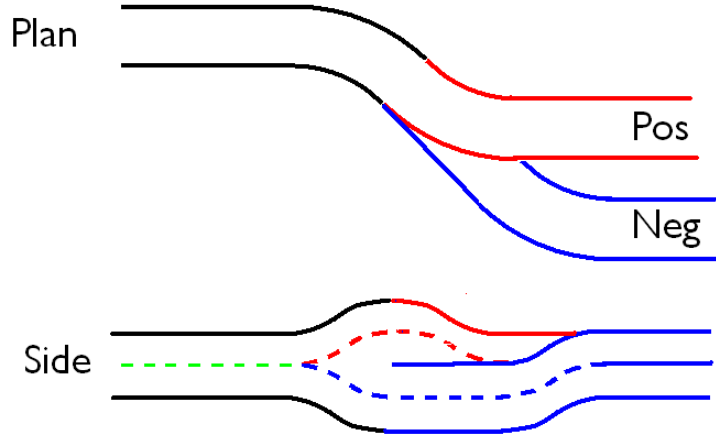


Figure 6: Charge separation method.

(from runprmw & param4pr)

	E1 MeV	E2 MeV	f MHz	cells	cavs	gap m	Lrf m	L m	$\mathcal{E}$ MV/m	Ppk MW	Ppktot MW	$t_{rf}$ $\mu s$	Pave MW	$P_{wal}$ MW	$N_{\mu}$ $10^{12}$
Drift	130	130	0	0	0	0.0	0	29	0.0	0.00	0.0	0	0.00	0.00	63
buncher	130	130	300	1	43	0.5	22	33	15.0	2.07	44.6	88	0.06	0.10	$12 \times 5$
rotation	130	130	210	1	44	0.5	22	33	16.0	4.03	177.4	150	0.40	0.66	$12 \times 3.5$
Totals	130	130		2	87		44	95			222		0.46	0.76	$12 \times 2.7$

As above, we estimate energy lost in the 4 K coils from fig. 13 from [1], requiring wall power of 3.3 MW to cool.

The cryostat static losses for the shorter length of 95 m, requires wall power  $95 \times 0.9/1000 = 0.009$  MW.

### 3.4 Charge Separation

#### 3.4.1 Neutrino Factory Charge Separation

In the Neutrino Factory case, separation of charges is not required until after transverse cooling and initial linac acceleration. By then, the beam is small and has a relatively small momentum spread. Separation then takes place naturally in dipoles forming part of the RLA injection chicane (A. Bogacz [6]).

#### 3.4.2 Muon Collider Charge Separation

To maximize cooling efficiency it appears best to cool straight away in all six dimensions. This may be possible without charge separation in a Helical FOFO Snake [5] (Y. Alexahin), but for the other schemes, RFOFO Guggenheim or HCC channel, the charges must be separated. For this study, we will assume the use of such systems requiring charge separation.

This initial separation, when the bunches have very large emittances, is non-trivial. The best method appears to be that using bent solenoids. An initial horizontal bend separates the charges vertically. A septum takes one sign and immediately bends it horizontally back to its original direction, removing its dispersion. The other sign is carried straight to separate it from the first sign, and then also bends back to the original direction, now displaced horizontally from the first sign.

Studies [16] have shown that doing it at the momentum of 230 MeV/c involves serious emittance blow up, but if the momentum is raised to 300 to 400 MeV/c, the performance can be quite good. The system uses no rf.

As an example we include the parameters for the 400 MeV/c case.

### Main Parameters

Momentum	p	400	MeV/c
Solenoid fields	B	1.9	T
Solenoid diameters	d	60	cm
Final beam separation	dy	2.1	m
Total length for positives	$L^+$	14.8	m
Total length for negatives	$L^-$	10.4	m

### Lengths and curvatures

Len m	$k$ $m^{-1}$
2.2	0.0807
0.8	0.1614
2.2	0.0807
(4.4)	0
2.2	-0.0807
0.8	-0.1614
2.2	-0.0807

### Performance

	Init	Neg	Pos	<incr> %
$\epsilon_{\perp}$ (mm)	15.1	15.2	15.3	1%
$\epsilon_{\parallel}$ (mm)	38.1	43.8	47.8	20%
$\sigma_{ct}$ (mm)	102	134	162	45%
Trans (%)	100	98	97	-2.5%

## 3.5 6D cooling

### 3.5.1 Introduction

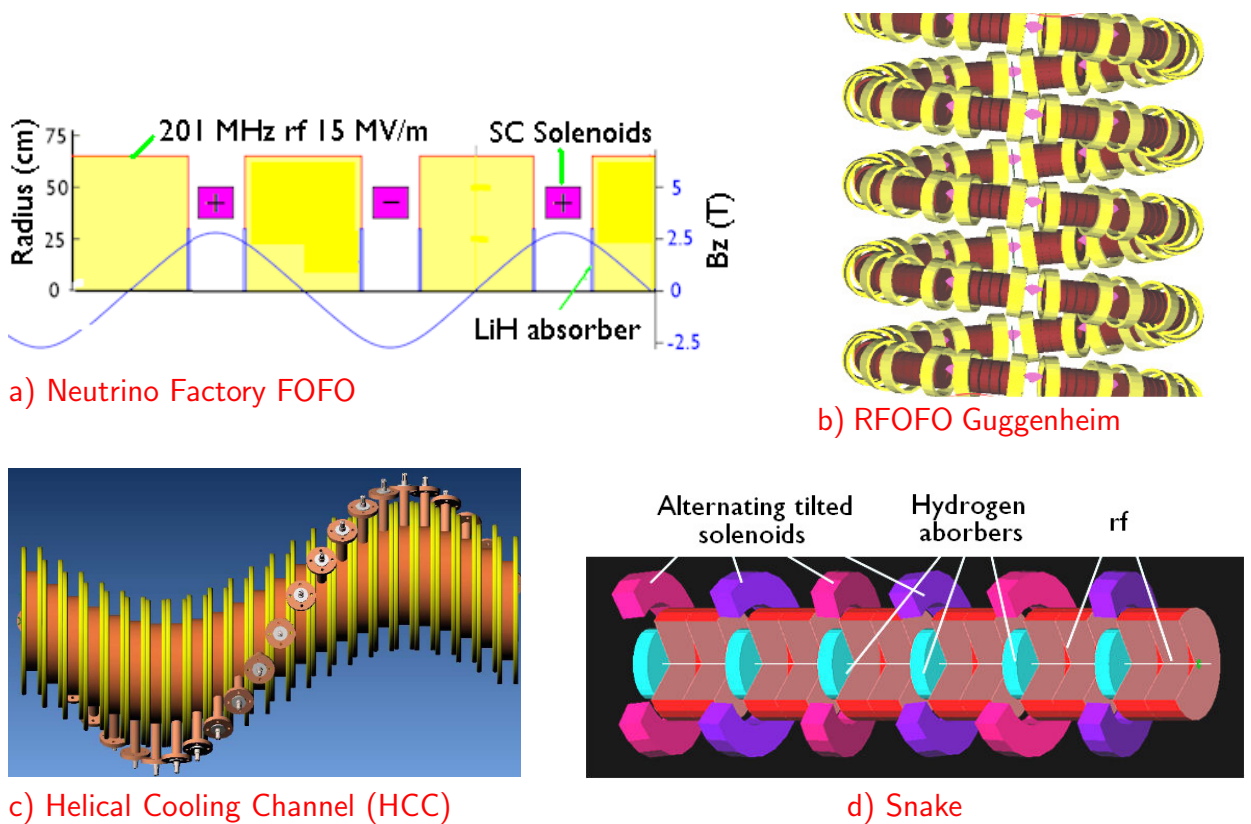


Figure 7: Cooling Lattices: a) Transverse FOFO ; b) 6D RFOFO Guggenheim c) 6D Helical Cooling Channel (HCC); d) 6D FOFO Snake

Four cooling schemes are illustrated in fig. 7. a) Shows a linear Focus-focus (FOFO) lattice as proposed for the Neutrino Factory. This lattice has no emittance exchange and cools only in the transverse dimensions. The other figures b) ,c), and d) show lattices with dipole fields that generate dispersion and emittance exchange. b) Shows a system of Reverse-Focus-Focus (RFOFO) lattices with tilted solenoids to give dipole field bending the lattice into a helical form (Guggenheim). Examples of the details of the lattices are given in Fig. 8. More detailed parameters for this scheme will be given below. c) shows the Helical Cooling Channel (HCC). It is a gas filled channel with the rf fully contained within helical

magnets. It achieves emittance exchange by having longer orbits, and thus more energy loss, for higher momentum particles. d) the FOFO Snake achieves emittance exchange by the higher momentum tracks passing through the plane parallel absorber slabs at larger angles.

The most complete parameters will be given for the RFOFO Guggenheim. Fewer for the HCC. No parameters are given for the Snake, whose use would be restricted to early stages to delay the need for charge separation until the emittances are lower and the use of 400 MeV/c is no longer required.

The 6D cooling for the Muon Collider is broken into two: the first is done using the full bunch train from the phase rotation; the second follows a bunch merging that combines these trains into single bunches: one of each sign.

### 3.5.2 Neutrino Factory: Transverse 4D Cooling

These parameters, though not part of the Muon Collider scheme, are included for comparison.

(from runprmw param4pc)

	E1 MeV	E2 MeV	f MHz	cells	cavs	gap m	Lrf m	L m	$\mathcal{E}$ MV/m	Ppk MW	Ppktot MW	$t_{rf}$ $\mu$ s	Pave MW	$P_{wal}$ MW	$N_{\mu}$ $10^{12}$
4D Cool	120	120	201	1	107	0.5	54	80	16.0	4.30	460.6	160	3.68	6.14	$21 \times 0.4$
Totals	120	120		1	107		54	80			461		3.68	6.14	$21 \times 0.25$

From fig. 13 in the Neutrino Factory IDR [1]: the energy lost in electrons  $\approx 25$  kW and in protons  $\approx 12$  kW. Not all this will be deposited in the coils and shielding should help. Assuming a reduction of a factor of two, the total is  $(25 + 12)/2 = 18.5$  kW. With a refrigerator efficiency at 20% of Carnot equaling 0.0027, the wall power =  $18.5 \text{ kW} / 0.0027 = 6.8$  MW

The cryostat static losses for 80 m require wall power  $80 \times 0.9/1000 = 0.07$  MW. The absorbers are LiH at room temperature, so no cryo load

### 3.5.3 Guggenheim Cooling

Since many of the lattices are common to the cooling before and after the merge, we list the parameters for all such lattices and then define which, and how many cells, are used in the two locations.

file in tapr	file in beta	$\beta$ cm	cell cm	rf f MHz	$\mathcal{E}$ MV/m	rf frac	abs L/2 cm	coil 1 z1-z2 cm	coil 1 r1-r2 cm	j A/mm <sup>2</sup>	$\hat{B}$ T	coil 2 z1-z2 cm	coil 2 r1-r2 cm	j A/mm <sup>2</sup>	$\hat{B}$ T	$B_o$ T	
041	rfoxb5	66	275	201	15.48	0.68	H	22.6	30.00-80.00	77.00-88.00	95.6	7.3				2.33	
042	rfoxb4	57	275	201	15.48	0.68	H	32.6	42.50-95.00	77.00-88.00	80.6	6.2				2.51	
043	rfoxb3	50	275	201	15.48	0.68	H	42.6	42.00-94.50	77.00-88.00	86.2	6.6				2.69	
044	rfoxb1	50	275	201	15.48	0.68	H	42.6	38.00-88.00	77.00-88.00	91.6	7.0				2.72	
045	rfoxb	39	275	201	15.48	0.68	H	42.6	30.00-80.00	77.00-88.00	95.6	7.3				2.75	
022	rfoxb12	34	235.7	235	15.48	0.68	H	36.5	12.86-30.00	42.86-51.43	68.3	5.1	25.72-94.29	66.00-74.58	75.7	5.1	3.08
023	rfoxb13	29	202.1	273	15.48	0.68	H	31.3	11.02-25.72	36.74-44.09	93.0	5.9	22.05-80.84	56.58-63.93	103.0	5.8	3.60
024	rfoxb14	25	173.2	319	15.48	0.68	H	26.8	9.45-22.05	31.50-37.80	126.5	6.9	18.90-69.30	48.51-54.81	140.1	6.7	4.20
025	rfoxb21	21	148.5	372	15.48	0.68	H	23.0	7.02-19.98	27.00-36.18	93.4	7.8	16.20-59.40	41.58-55.08	86.3	8.0	4.91
026	rfoxb22	18	127.3	435	15.48	0.68	H	19.7	6.02-17.13	23.15-31.01	127.2	9.0	13.89-50.92	35.64-47.22	117.5	9.5	5.73
027	rfoxb23	18	109.1	507	15.48	0.68	H	16.9	5.16-14.68	19.84-26.59	173.1	10.6	11.90-43.65	30.55-40.47	159.9	10.9	6.68
028	rfoxb31	13	93.55	591	15.48	0.68	H	14.5	4.42-12.59	13.61-26.20	102.7	11.1	10.21-37.42	26.20-46.61	123.0	13.5	7.80
029	rfoxb32	11	80.20	690	15.48	0.68	H	12.4	3.79-10.79	11.66-22.45	139.8	14.7	8.75-32.08	22.45-39.95	167.4	15.7	9.10
030	rfoxb33	10	68.75	805	15.48	0.68	H	10.6	3.25-9.25	10.00-19.25	190.2	15.8	7.50-27.50	19.25-34.25	227.7	18.4	10.6
031	rbk7a2	8.2	68.75	805	15.48	0.68	H	10.6	2.50-9.25	9.25-19.25	276.0	15.7	10.50-28.00	19.25-34.25	222.2	17.3	10.9
032	rbk8b	6.9	68.75	805	20.05	0.5	H	10.6	3.25-12.50	10.00-19.25	217.7	18.0	3.25-22.00	19.25-34.25	203.1	18.0	11.8
033	rbk8c	5.9	68.75	805	20.05	0.5	H	10.6	3.25-12.50	10.00-19.25	287.8	20.0	3.25-19.50	19.25-34.25	191.4	20.0	12.3
034	rbk8d	4.9	68.75	805	20.05	0.5	H	10.6	3.25-12.50	7.00-21.25	239.7	18.5	13.25-23.25	19.25-34.25	163.8	12.0	13.1
035	rbk8e2	4.1	68.75	805	20.05	0.5	LH	1.9	3.25-12.50	6.50-21.75	259.7	19.4	13.25-23.25	19.25-29.25	133.2	12.0	13.9
036	rbk8f2	3.4	68.75	805	20.05	0.5	LH	1.9	3.00-13.00	6.50-21.75	291.9	20.8					14.8
037	rbk8g2	2.8	68.75	805	20.05	0.5	LH	1.9	2.50-13.00	4.88-19.63	257.5	19.2					15.8

Before the merge the simulation (run tapr7g) uses the following numbers of the cells with parameters corresponding to the numbers given above.

Cells	12	10	8	8	8	8	9	11	12	15	17	20	24	65	40	80	347
Files	41	42	43	44	45	22	23	24	25	26	27	28	29	30	31	32	16

The total length of hydrogen is 112 m. With energy loss per meter of  $dE/dx = 29$  MeV/m, and average beam intensity  $21 \times 10^{12}$ , and repetition rate of 15 Hz, then the total power dissipated in the hydrogen is given by:

$$\text{Power at 20 K} = 112 \times 29 \times 10^6 \times 21 \times 10^{12} \times 1.6 \times 10^{-19} \times 15 = 0.16 \text{ MW}$$

With our assumed cryogenic efficiency of 20% of the Carnot efficiency of  $0.2 \times 20/293 = 1.4\%$ , the wall power to cool the hydrogen is  $0.16/1.4\% = 11.4$  MW

The simulation (run [tapr12f](#)) after the merge used:

Cells	8	8	9	11	12	15	17	20	24	40	40	40	40	40	51	20	584	
Files	45	22	23	24	25	26	27	28	29	30	31	32	33	34	35	36	37	17

The total length of of hydrogen is 93 m. With energy loss per meter of  $dE/dx = 29$  MeV/m, and average beam intensity  $8 \times 10^{12}$ , and repetition rate of 15 Hz, then the total power dissipated in the hydrogen is given by:

$$\text{Power at 20 K} = 93 \times 29 \times 10^6 \times 8 \times 10^{12} \times 1.6 \times 10^{-19} \times 15 = 0.05 \text{ MW}$$

With our assumed cryogenic efficiency of 20% of the Carnot efficiency of 1.4 %, the wall power to cool the hydrogen is  $0.05 / 1.4\% = 3.6$  MW

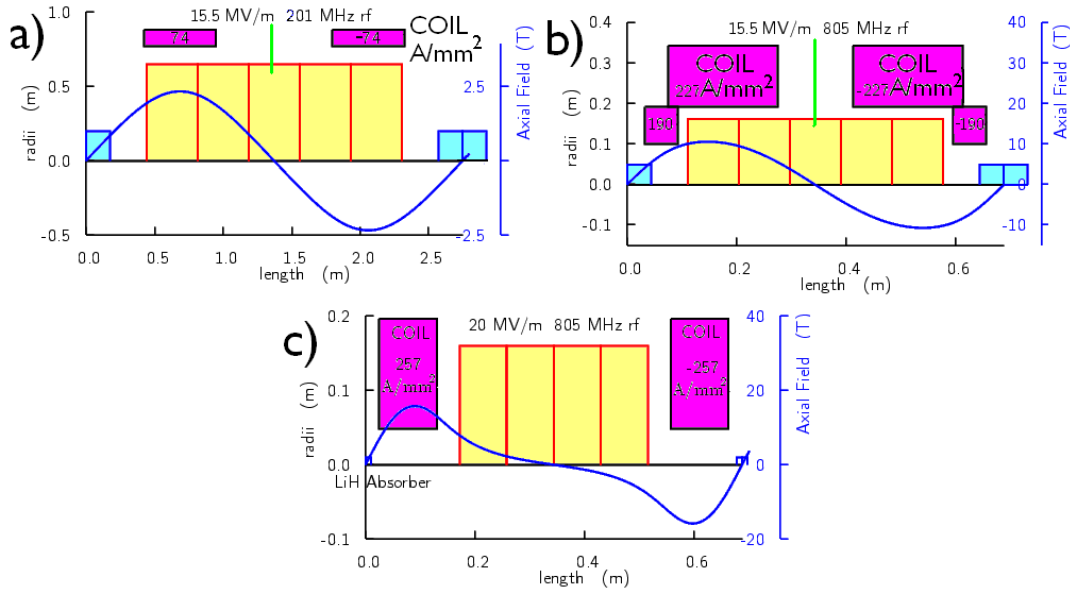


Figure 8: Examples of lattice used in Guggenheim 6D cooling: a) First 201 MHz FOFO lattice # 41; b) A typical 805 MHz RFOFO lattice # 27; c) The last RFOFO lattice # 37.

Fig. 8 shows the dimensions of the solenoid coils, rf, and liquid hydrogen absorbers for three lattice examples. Initially, in order to obtain the widest momentum acceptance,  $\pm 32\%$ , the very early lattices use symmetrically space alternating field solenoids (FOFO for Focus-Focus). The frequencies used are low (201 MHz), and the cell relatively long (2.75 m). Later in the cooling, the frequencies rise to 805 MHz and the cells are shorter (0.6875 m). The later lattices, like that shown in fig. 8b, are bi-periodic

(SFOFO for Super-Focus-Focus) giving lower betas, but somewhat less momentum acceptance ( $\pm 22\%$ ). The final lattice used in this design, #37 shown in fig. 8c, has the same cell length, but fields tuned to minimize the beta at the cost of lowering the momentum acceptance,  $\pm 12\%$ .

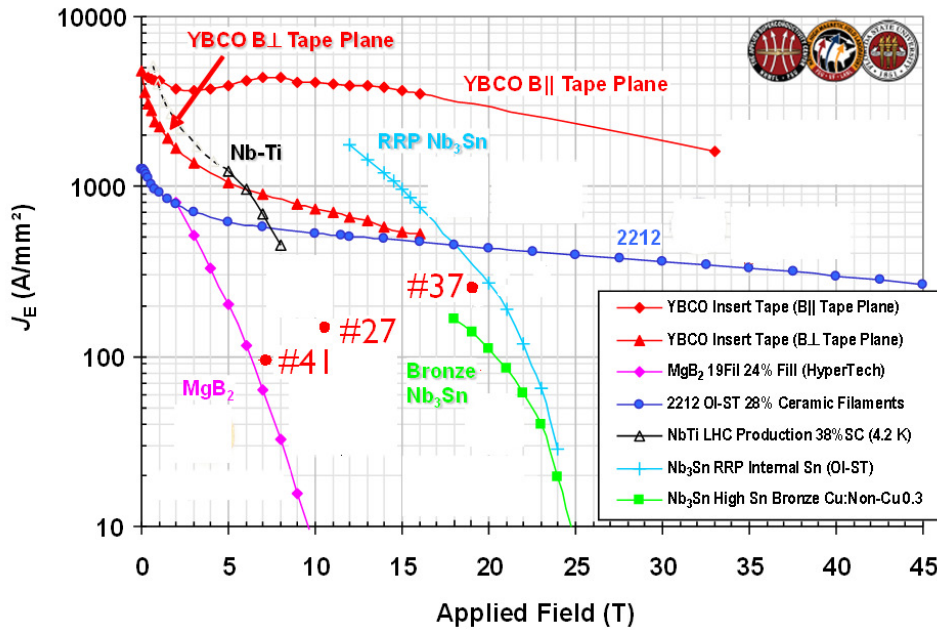


Figure 9: Superconductor engineering current densities vs. local magnetic fields for different materials, with the requirements for the three examples shown in figure 8.

Figure 9 shows the required engineering current densities for these examples. It is seen that the early lattices, like #41 is well within Nb-Ti specifications. Later lattices, like #27, are well within Nb3Sn specifications. The last stage, #37, is barely within Nb3Sn specifications and probably needs 2 K operation or HTS conductors.

The following table gives an estimate for rf power requirements for Guggenheim 6D cooling before merge.

(from `tapr7g` & `runprmw param4g`)

	E1	E2	f	cells	cavs	gap	Lrf	L	$\mathcal{E}$	Ppk	Ppktot	$t_{rf}$	Pave	$P_{wall}$	$N_{\mu}$
	MeV	MeV	MHz			m	m	m	MV/m	MW	MW	$\mu s$	MW	MW	$10^{12}$
H2 6D Cool	0.130	0.130	201	46	184	0.5	86	126	15.5	4.04	743.4	160	1.78	2.97	$21 \times 1.3$
H2 6D Cool	0.130	0.130	402	40	213	0.2	50	74	15.5	1.43	304.2	57	0.26	0.43	$21 \times 1.0$
H2 6D Cool	0.130	0.130	805	141	740	0.1	86	120	15.5	0.50	373.0	20	0.11	0.19	$21 \times 0.9$
Totals	0.39	0.130		227	1137		222	320			1421		2.15	3.59	$21 \times 0.66$

Since 6D cooling with a Guggenheim lattice works with only one of the two signs, the total rf Wall Power is  $2 \times 3.59 = 7.2$  MW

Numbers of muons  $N_{\mu}$  given above for multiple bunches are the total divided by number of bunches. The actual numbers per bunch vary greatly. The number of bunches given for this simulation is 21, although the number is more likely to be  $\approx 12$  in future simulations. Most of the beam loss seen in IDR simulation was early in cooling and we will assume they are the same for this 6D cooling.

From fig. 13 in the IDR: the energy lost in electrons is  $\approx 25$  kW, and the energy lost in protons is  $\approx 12$  kW.

Not all this will be deposited in the coils and shielding should be added, so we will assume that these losses can be halved: giving  $(25+12)/2=18.5$  kW. With efficiency of 20% Carnot efficiency at 4 K of 0.0027, the wall power to remove this deposited energy will be  $18.5 \text{ kW}/0.0027 = 6.8$  MW. In addition there will be heat leaks into the cryogenic system which we estimate from the total length of 320 m at 4 K: requiring wall power to cool of  $2 \times 320 \times 0.9/1000 = 0.58$  MW

For the Guggenheim Cooling rf after the merge we estimate:

	E1 MeV	E2 MeV	f MHz	cells	cavs	gap m	Lrf m	L m	$\mathcal{E}$ MV/m	Ppk MW	Ppktot MW	$t_{rf}$ $\mu\text{s}$	Pave MW	$P_{wal}$ MW	$N_{\mu}$ $10^{12}$
H2 6D Cool	0.130	0.130	201	8	32	0.5	15	22	15.5	4.04	129.3	160	0.31	0.52	9.7
H2 6D Cool	0.130	0.130	402	40	213	0.2	50	74	15.5	1.43	304.2	57	0.26	0.43	9.3
H2 6D Cool	0.130	0.130	805	156	800	0.1	93	131	15.5	0.50	403.2	20	0.12	0.20	8.4
H2 6D Cool	0.130	0.130	805	120	360	0.1	46	83	19.0	0.76	272.7	20	0.08	0.14	6.4
LiH 6D Cool	0.130	0.130	805	104	312	0.1	40	72	19.0	0.76	236.3	20	0.07	0.12	5.5
Totals	0.650	0.130		428	1717		243	381			1346		0.84	1.40	4.7

For both signs the total rf power after the merge is  $2 \times 1.4 = 2.8$  MW. In addition there are the static losses for the two 381 m systems at 4 K leading to wall power  $2 \times 381 \times 0.9/1000 = 0.68$  MW.

A preliminary study of space charge effects has shown serious longitudinal space charge effect towards the end of the 6D cooling after the merge. A modified design has been proposed that avoids these problems, but more work and simulation is required.

### 3.5.4 Helical Cooling Channel (HCC)

		HCC	RFOFO	
Muon Momentum	p	200	207	MeV/c
Ave Hydrogen density	$\rho_{H2}$	0.013	0.011	gm/cm <sup>2</sup>
Gas pressure	P	20	1	Atm.
Absorber temperature	T	30	20	Deg Kelvin
rf gradient	$\mathcal{E}$	28	15.5	MV/m
rf gradient along beam	$\mathcal{E}(s)$	19.8	15.5	MV/m
Ave beam gradient	$\mathcal{E}_s$	19.8	10.5	MV/m
rf phase	$\phi$	20	32	deg.

Some basic parameter of the HCC and RFOFO Guggenheim are given above. In the HCC case the average density is just the local gas density. The rf gradient along the beam is the local gradient in the cavities (along z) times the sine of the pitch angle (approximately 45 deg.)

In the RFOFO case the average density is the liquid density times the typical fraction (15.5%) of absorber. This fraction is less at the start and end of the channel, but this "typical" fraction is constant for most stages. The average rf gradient is the local cavity gradients times the fraction (68%) of rf cavity along the axis. Towards the end of the lattice, this fraction is somewhat less, but the gradient is there raised to keep the same average.

Simulated performances of a HCC and a comparable RFOFO Guggenheim channel are show in fig. 10. Neither simulation included bunch merging, so neither corresponds to the actual parameters of the collider. The HCC simulation used ideal helical magnetic fields given in the following table, and included no aperture restrictions. The Guggenheim simulation uses matrices to represent the emittance exchange, rather than actual curved orbits and wedge absorbers. So neither represents fully accurate representation of a true systems, but perhaps some general conclusions may be valid.

The average performances of the two systems, over a wide range of emittances are quite similar, with the HCC cooling slightly faster, as would be expected from its slightly greater average hydrogen density

(0.013 vs. 0.011). The HCC yields relatively lower longitudinal emittances, presumably from the choice of stronger emittance exchange. The HCC also has somewhat better transmission, probably because of its higher rf gradients and thus lower rf phase angle. An HCC simulation [20] using 201, 402 & 805 MHz rf and the lower rf gradient of 17 MV/m, instead of 28 MV/m did, as expected, have a lower transmission (38% vs. 60%).

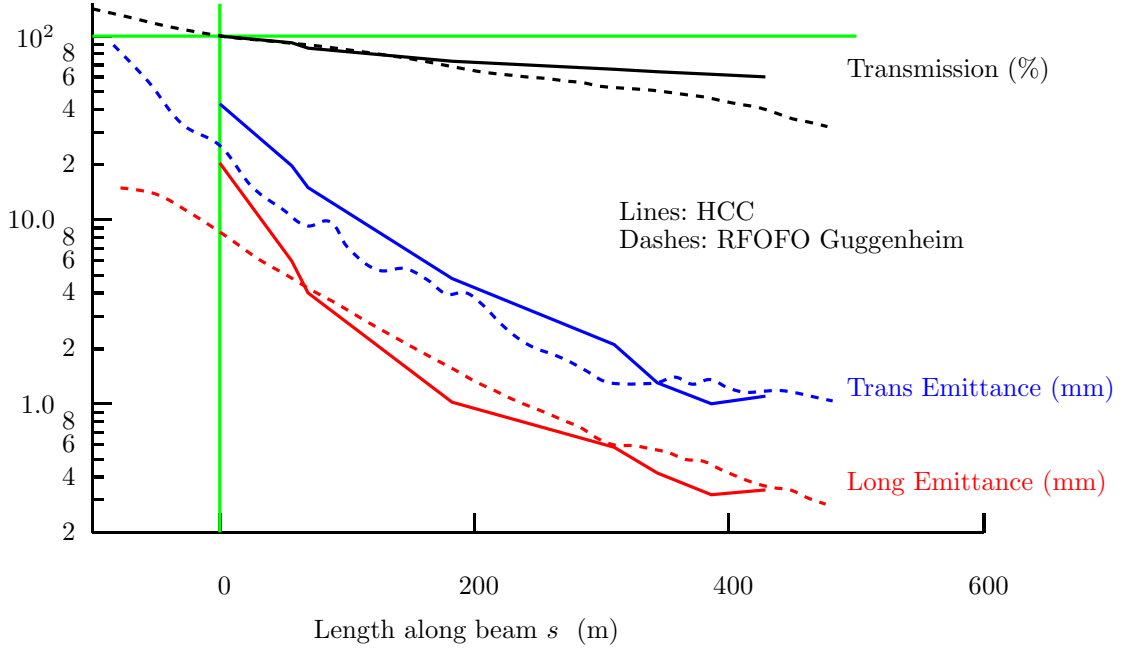


Figure 10: Simulated performances of an HCC channel compared with that of an RFOFO Guggenheim channel. In neither case is any bunch merging included. Transmission, and emittances are plotted against length  $s$  along the beams - not along the helix axes. The scale in  $s$  in the Guggenheim case has been displaced by 100 m, and its transmissions renormalized, to show the simulations at similar emittances.

The following table gives some parameters of the fields and performance of the stages used in the simulation shown in fig. 10.

stages	$z$ m	$b_1$ T	$b'$ T/m	$B_z$ T	$\lambda$ m	$f$ MHz	$\epsilon_{\perp}$ mm	$\epsilon_{\parallel}$ mm	transm.
1	0	0	0	0	0	0	20.4	42.8	1.0
2	40	1.3	-5	-4.2	1	325	5.97	19.7	.92
3	49	1.4	-6	-4.8	.9	325	4.01	15	.86
4	129	1.7	-8	-5.2	.8	325	1.02	4.8	.73
5	219	2.6	-2	-8.5	.5	650	.58	2.1	.66
6	243	3.2	-3.1	-9.8	.4	650	.42	1.3	.64
7	273	4.3	-5.6	-14.1	.3	650	.32	1	.62
8	303	4.3	-5.6	-14.1	.3	1300	.34	1.1	.6

Stage 1 is a matching stage.  $b_1$  is the transverse dipole field that is rotating azimuthally with a pitch of  $\lambda$ ;  $b'$  is the transverse field gradient that rotates with the same pitch;  $B_z$  is the axial field and  $f$  is the rf frequency.

The published coil details for the initial matching and two of the 7 stages are given below. Similar details for stages 3,4,and 5 are presumably obtainable from interpolations between stages 2 and 6. Stages 7 and 8 are recognized to be more challenging and have not yet been defined.

stage	$R_c$ m	$\lambda$ m	$B_z$ T	R1 m	R2 m	n	$L_c$ m	j A/mm <sup>2</sup>	L m
1	0 → 0.28	1.9	0.55	0.35	0.4	20	0.025	220 → 194	5.5
2	.28	1	.55	.35	.4	20	.025	194	
6	.16	.4	6.73	.18	.28	20	.01	332.9	

$R_c$  are the radii of the coil centers as they step around the helix with wave length  $\lambda$ .  $B_z$  is an axial field provided by an outer solenoid (dimensions unspecified). R1 and R2 are the inner and outer radii of the coils. In each helix length there are n coils, each with length  $L_c$ .  $j$  is the current density in these coils.

### 3.6 Bunch Merging

Several merging schemes have been discussed. Two of these, one of 21 bunches [17] and one for  $\approx 12$  bunches [18], merged in only the longitudinal dimensions. The second of these used a helical drift lattice (similar to those used in the HCC) that gave a linear relation between particle slip and momentum. The one [19] whose parameters are given here merged 21 bunches in all 6 dimensions, generating a merged beam that matches more naturally back into the cooling lattice. It uses a planar dipole wiggler for the drift. A new design, combining 12 bunches in 6 dimensions, using a helical drift lattice, is being developed and appears to have significantly better performance than the one given here.

#### 3.6.1 Muon Collider 6D Merge of 21 bunches

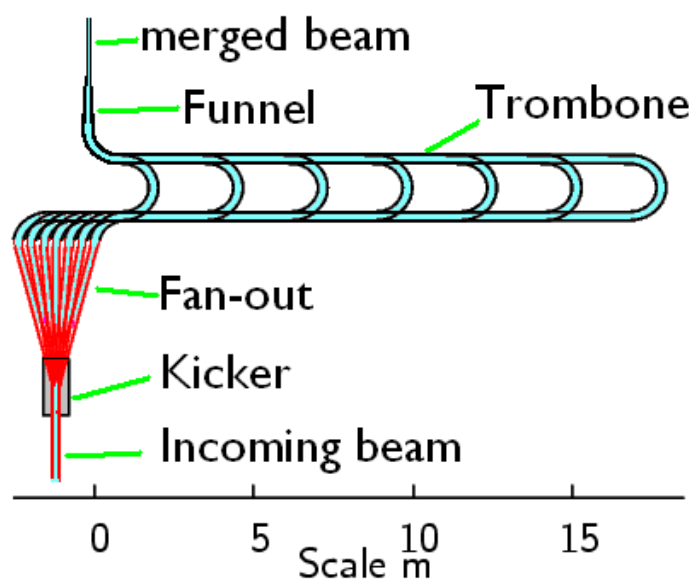


Figure 11: Schematic of the 6D bunch merging scheme

(from runprm param4m)

	E1 MeV	E2 MeV	f MHz	cells	cavs	gap m	Lrf m	L m	$\mathcal{E}$ MV/m	Ppk MW	Ppktot MW	$t_{rf}$ $\mu s$	Pave MW	$P_{wal}$ MW	$N_{\mu}$ $10^{12}$
Drift	130	130						10				0			$21 \times 0.63$
rotate	130	130	201	27	27	0.3	9	10	5.0	0.42	5.7	160	0.01	$2 \times 0.02$	$21 \times 0.63$
chirp	130	130	67	3	3	1.0	3	3	5.0	2.18	3.3	831	0.04	$2 \times 0.07$	$21 \times 0.63$
wiggler	130	130						45				0			$21 \times 0.63$
kicker	130	130						8				0			$21 \times 0.63$
trombone	130	130						20				0			$21 \times 0.52$
chirp	130	130	30	6	6	1.5	9	6	2.0	1.17	3.5	2775	0.15	$2 \times 0.24$	11.0
Drift	130	130						14				0			11.0
Totals	130	130		36	36		21	115			12		0.20	0.66	11.0

Numbers of particles  $N_{\mu}$  given for multiple bunches are the total divided by number of bunches. The actual numbers per bunch vary greatly. The total rf wall Power is  $2 \times 0.66 = 1.32$  MW. Static cryostat losses for  $2 \times 115$  m, requires wall power =  $230 \times 0.9/1000 = 0.2$  MW

### 3.7 Muon Collider Final 4D Cooling

#### 3.7.1 Introduction

Final cooling sequences have been designed using maximum fields of 30,40 and 50 T [21], with performance improving with the field. These results suggest that the collider specified emittances would be achieved with 35 T magnets. The parameters given here assume 40 T and modestly exceed the requirements.

Matching and reacceleration between high field magnets has only been designed in one case: between the last two high field magnets. Simulation of this one case gave performance within the range assumed in the design sequence.

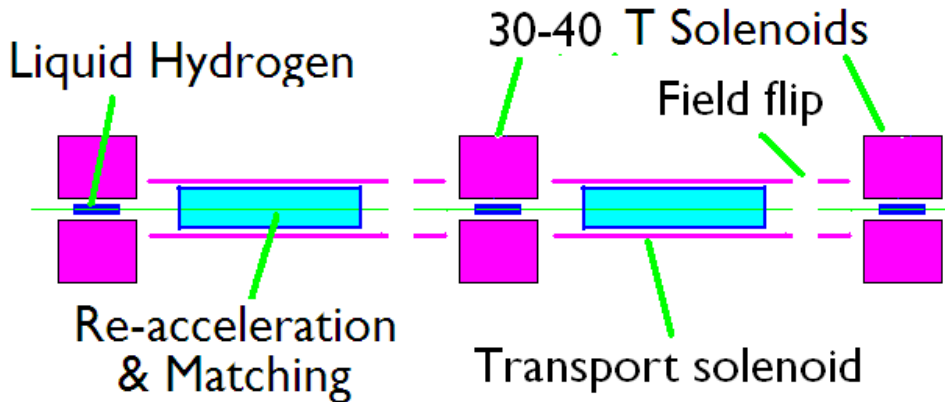


Figure 12: Schematic of final transverse cooling in high field solenoids.

#### 3.7.2 rf parameters of stages

from depend10

	E1 MeV	E2 MeV	cell m	B T	H <sub>2</sub> L cm	Mag L m	bore r cm	acc L m	freq MHz	grad MV/m	Ppk MW	t <sub>rf</sub> μs	Pwall MW
NCRF	66.1	66.6	3.19	40	77.5	1.78	3.2	2.1	201	15.0	20.2	160.0	≈0.08
NCRF	66.6	66.9	3.17	40	77.3	1.77	3.0	2.1	201	15.0	20.3	160.0	≈0.08
NCRF	66.9	67.1	3.25	40	75.0	1.75	2.8	2.1	201	15.0	19.7	160.0	≈0.08
LFRF	67.1	54.5	3.43	40	75.0	1.75	2.7	1.7	153	10.7	16.6	139.5	≈0.06
LFRF	54.5	41.3	3.26	40	53.5	1.53	2.6	1.5	110	7.1	14.4	118.6	≈0.04
LFRF	41.3	32.4	3.12	40	31.8	1.32	2.6	1.7	77	4.5	16.0	98.7	≈0.04
LFRF	32.4	25.7	3.15	40	20.6	1.21	2.5	1.9	52	2.8	17.8	81.7	≈0.04
LFRF	25.7	20.7	3.59	40	12.9	1.13	2.5	2.6	31	1.5	24.6	62.9	≈0.04
Induction	20.7	16.2	4.39	40	9.7	1.10	2.4	2.8	18	1.0	52.7	47.2	2×≈0.06
Induction	16.2	12.2	5.79	40	6.9	1.07	2.4	2.0	9	1.0	179.2	34.4	2×≈0.15
Induction	12.2	11.1	5.81	40	4.3	1.04	2.4	3.8	6	1.0	931.2	28.3	2×≈0.66
Induction	11.1	11.2	6.32	40	3.6	1.04	2.3	4.5	5	1.0	2337.6	24.3	2×≈1.42
Totals	66.1	11.2	0.00	40	448	16.48		28.8			3650.2		≈2.75

The length of this final cooling is 78 m. The rf wall power = 5.42 MW (or half that if charges combined). Static cryogenic losses are estimated as  $100 \times 0.9/1000 = 0.09$  MW

The average number of muons cooled is, for both signs:  $N_\mu \approx 2 \times 4 \times 10^{12} = 8 \times 10^{12}$ . The total energy lost in hydrogen per muon is 160.8 MeV. So the energy deposited in the hydrogen is:

$$\text{Power at 20 K} = 160.8 \times 10^6 \times 8 \times 10^{12} \times 1.6 \times 10^{-19} \times 15 = 3090 \text{ W}$$

$$\text{Wall power for cryo at 20 K, } P_{wall} = 3.09 \text{ kW}/0.014 = 0.22 \text{ MW.}$$

A preliminary study of space charge effect in the final cooling has shown serious transverse effect toward the start of the sequence. These problems appear solvable by increasing the focus fields in the transport between high field magnets from 1 T to about 3 T.

### 3.7.3 Room Temperature Acceleration from 6 to 400 MeV

The sequence of initial acceleration is constrained by the large longitudinal emittances giving initially very long bunches, but becomes more reasonable as the energy rises. Thus the initial acceleration uses induction linacs, followed by low frequency cavities.

The following are only very approximate estimates with no simulation  
(from Depend10)

	E1 MeV	E2 MeV	Len m	typ	Freq MHz	grad MV/m	θ deg	<grad> MV/m	Decay %	P <sub>peak</sub> MW	t <sub>rf</sub> ms	Pwall MW	N <sub>μ</sub> 10 <sup>12</sup>
Induction	6.7	13.4	6.7	Ind	5.3	1.0	30	1.0	2.5	1.2		2 × 0.27	3.3
Induction	13.4	26.7	13.3	Ind	10.3	1.0	30	1.0	3.4	0.8		2 × 0.56	3.2
Induction	26.7	53.1	26.4	Ind	19.5	1.0	30	1.0	4.6	0.6		2 × 1.06	2.9
Linac	53.1	105.7	30.0	RTRF	35.9	1.8	30	1.8	3.5	1.4	2.1	0.1	2 × 2.8
Linac	105.7	210.3	28.8	RTRF	64.4	3.6	30	3.6	2.1	4.4	0.9	0.1	2 × 2.7
Linac	210.3	418.4	28.0	RTRF	113.9	7.4	30	7.4	1.2	13.9	0.4	0.1	2 × 2.7
Totals	6.7	832.7	133.2						16.2	25.0		4.08	

The transmission 86.7 %. The total wall power for rf = 4.1 MW. The wall power to cool cryostat static losses for 103 m is  $103 \times 0.9/1000 = 0.09$  MW.

### 3.8 Super-Conducting Acceleration

#### 3.8.1 Neutrino Factory Acceleration with FFAG

For comparison with the acceleration designs for the Muon Collider, we give some parameters for the IDS Neutrino factory.  $L_{rf}$  is the total length of rf cavities in each section.  $L_{arc}$  is the sum of lengths of the dog-bone arcs. The number of turns reflects the number of beam passes through the linac. The fractional turns arise because of injection in the center of the linac.  $\theta$  is the rf phase angle measured from the maximum.  $Decay$  gives the % loss in each section.  $P_{peak}$  is the total peak rf power in each stage,  $t_{rf}$  is the rf pulse length.  $P_{ave}$  is the time average rf power used.  $P_{wall}$  is the average wall power used for rf assuming a 60% klystron and power supply efficiency.  $N_\nu$  is the average muon flux through that section.

(From param3z0)

	E1 GeV	E2 GeV	Linac m	$L_{rf}$ m	$L_{arc}$ m	turns	typ	Cav's	Freq MHz	Lcav m	grad MV/m	$\theta$ deg	<grad> MV/m	Decay %	$P_{peak}$ MW	$t_{rf}$ ms	$P_{ave}$ MW	$P_{wall}$ MW	$N_\nu$ $10^{12}$
Linac	0.16	0.22	18	4	0	1.0	SCRf	4	201	0.75	17	18	3.3	1.0	2.0	3.0	0.3	0.5	1.0
Linac	0.22	0.40	40	11	0	1.0	SCRf	14	201	0.75	17	18	4.5	1.6	7.1	3.0	1.1	1.8	1.0
Linac	0.4	0.90	88	31	0	1.0	SCRf	41	201	0.75	17	18	5.7	1.9	20.8	3.0	3.1	5.2	1.0
RLA	0.9	3.60	79	37	772	4.5	SCRf	49	201	0.75	17	18	2.4	8.2	24.9	3.0	3.7	6.2	$5 \times 0.9$
RLA	3.6	12.50	264	122	1544	4.5	SCRf	163	201	0.75	17	18	3.3	5.7	82.8	3.0	12.4	20.7	$5 \times 0.9$
FFAG	12.5	25.00	521	86	0	9.0	SCRf	114	201	0.75	17	18	2.7	4.1	57.9	3.0	8.7	14.5	$9 \times 0.8$
	0.16	25.00	1010	291	2316			385						20.8	196		29.3	48.9	0.8

The rf wall power consumption is relatively high (48.9 MW) because of the high repetition rate of 50 Hz, compared with 15 Hz for the Muon Collider. But the transmission is relatively good (79.2%).

The following table gives details of the two dog-bone RLAs. The arcs, in this case, are as designed by Alex Bogacz [6]. Note that the linac lengths for the first passes are shorter than subsequent ones in order to avoid too large a phase slip. This is achieved by injecting into the linac half way along its length.

(From paramz0)

	E1 GeV	E2 GeV	dE GeV	L m	slip deg	$\mathcal{E}$ MV/m	Decay %
linac	0.90	1.20	0.30	39.5	41	7.59	0.55
arc	0.90	1.20		130.0		2.31	1.59
linac	1.20	1.80	0.60	79.0	43	7.59	0.80
arc	1.20	1.80		172.0		3.49	1.44
linac	1.80	2.40	0.60	79.0	23	7.59	0.58
arc	1.80	2.40		214.0		2.80	1.37
linac	2.40	3.00	0.60	79.0	14	7.59	0.45
arc	2.40	3.00		256.0		2.34	1.32
linac	3.00	3.60	0.60	79.0	9	7.59	0.37

	E1 GeV	E2 GeV	dE GeV	L m	slip deg	$\mathcal{E}$ MV/m	Decay %
linac	3.60	4.59	0.99	132.0	10	7.49	0.51
arc	3.60	4.59		260.0		3.80	0.89
linac	4.59	6.57	1.98	264.0	12	7.49	0.75
arc	4.59	6.57		344.0		5.75	0.83
linac	6.57	8.54	1.98	264.0	6	7.49	0.56
arc	6.57	8.54		428.0		4.62	0.79
linac	8.54	10.52	1.98	264.0	4	7.49	0.44
arc	8.54	10.52		512.0		3.86	0.77
linac	10.52	12.50	1.98	264.0	3	7.49	0.37

#### 3.8.2 Muon Collider Acceleration with FFAG

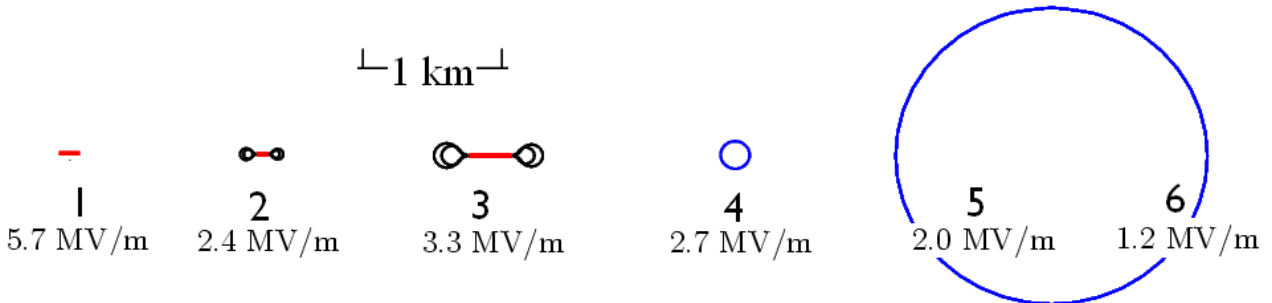


Figure 13: Scale dimensions of first design of acceleration systems including an FFAG.

This represents a straightforward extension of the acceleration designed for the Neutrino Factory. The energies of Linacs and FFAG are raised to allow the larger longitudinal emittance to be accepted. The final Rapid Cycling Synchrotrons (RCS) are as proposed by Don Summers [7].

(From param3z1)

	E1 GeV	E2 GeV	Linac m	Lrf m	Larc m	turns	Cav's	Freq MHz	Lcav m	grad MV/m	$\theta$ deg	<grad> MV/m	decay %	P <sub>peak</sub> MW	t <sub>rf</sub> ms	P <sub>ave</sub> MW	P <sub>wall</sub> MW	N <sub><math>\mu</math></sub> 10 <sup>12</sup>
Linac	0.40	1.20	140	49	0	1.0	65	201	0.75	17	18	5.7	2.7	33.0	3.0	1.5	2.5	3.3
RLA	1.20	4.20	79	37	870	5.0	49	201	0.75	17	18	2.4	7.4	24.9	3.0	1.1	1.9	5 × 3.2
RLA	4.20	15	288	134	1832	5.0	178	201	0.75	17	18	3.3	5.6	90.4	3.0	4.1	6.8	5 × 3.0
FFAG	15	30	622	103	0	9.0	137	201	0.75	17	18	2.7	4.1	69.6	3.0	3.1	5.2	9 × 2.8
RCS	30	400	6683	556	0	28.0	2925	805	0.19	25	18	2.0	19.0	400.9	0.6	3.5	5.9	2 × 28 × 2.7
RCS	400	750	6683	335	0	44.0	1760	805	0.19	25	18	1.2	8.1	241.2	0.9	3.3	5.5	2 × 44 × 2.2
	0.16	750	14495	1214	2702		5114						39.2			16.7	27.8	2.0

Wall power for rf = 27.8 MW at 15 Hz

Transmission = 60.8%. But with early room temperature acceleration, it is only 52.7 %, which, when compared with our original target of 70%, was deemed unacceptable.

The following table gives details of the two dog-bone RLAs. The arcs lengths here are taken from the linear fit to Alex Bogacz's designs shown in fig. 2.

(From paramz1)

	E1 GeV	E2 GeV	dE GeV	L m	slip deg	$\mathcal{E}$ MV/m	Decay %
linac	1.20	1.80	0.60	79.0	43	7.59	0.80
arc	1.20	1.80		173.8		3.45	1.46
linac	1.80	2.40	0.60	79.0	23	7.59	0.58
arc	1.80	2.40		204.8		2.93	1.31
linac	2.40	3.00	0.60	79.0	14	7.59	0.45
arc	2.40	3.00		232.9		2.58	1.20
linac	3.00	3.60	0.60	79.0	9	7.59	0.37
arc	3.00	3.60		259.0		2.32	1.12
linac	3.60	4.20	0.60	79.0	7	7.59	0.32

	E1 GeV	E2 GeV	dE GeV	L m	slip deg	$\mathcal{E}$ MV/m	Decay %
linac	4.20	6.36	2.16	288.0	14	7.50	0.87
arc	4.20	6.36		361.6		5.97	0.90
linac	6.36	8.52	2.16	288.0	7	7.50	0.62
arc	6.36	8.52		429.9		5.02	0.80
linac	8.52	10.68	2.16	288.0	4	7.50	0.48
arc	8.52	10.68		491.6		4.39	0.73
linac	10.68	12.84	2.16	288.0	3	7.50	0.39
arc	10.68	12.84		548.5		3.94	0.68
linac	12.84	15.00	2.16	288.0	2	7.50	0.33

The Rapid Cycling Synchrotrons (RCS) are pulsed at the main repetition rate of 15 Hz. For the first RCS, both quadrupoles and dipoles rise time is the same, corresponding to a frequency of 260 Hz. For the second ring, while the quadrupoles ramp with the beam momentum at 150 Hz, the dipoles are pulsed at a higher frequency, 550 Hz, starting at full field opposed to the interleaved super-conducting dipoles, and ending with the opposite polarity, now helping the super-conducting dipoles.

The pulsed magnets are made of thin laminated grain oriented steel. The windings would be of 2 mm copper wire. Summers estimated total power consumption at 15 Hz of 2.3 MW. The breakdown of loss was: 38% eddy-current in steel, 28% resistive losses, and 15% for hysteresis.

For beam parameters the assumption was to use essentially the same lattice as the TeVatron.

		RCS 1	RCS 2
vertical beta	m	99	99
minimum energy	GeV	30	400
6 sigma beam height	mm	18	4.8
width	mm	30	50
Core loss	W/kg	11	40
Weight of Fe	Tons	550	780
Core loss	kW/ring	260	1200
Quad length	m	1.7	3.2
Quad gradient	T/m	30	30
Quad frequency	Hz	260	150
Pulsed dipole lengths	m	6.3	3.75/7.5/3.75
Pulsed dipole field	T	1.8	1.8
Pulsed dipole frequency	Hz	160	550
Super-conducting dipole lengths	m	-	2 × 4.2

### 3.8.3 Acceleration with improved transmission

In order to improve the transmission we made the following changes:

- RLA 1: Increased acceleration length (306 m), relative to the arc lengths (210-413), to increase the average accelerating gradient.
- RLA 2: Again with a relatively long linac 1250 (cf arcs 698-1716), now going to a higher energy.
- No FFAG
- Injection to first RLA at 100 GeV, instead of 30 GeV
- More rf in RCS2 and more rapid ramp.

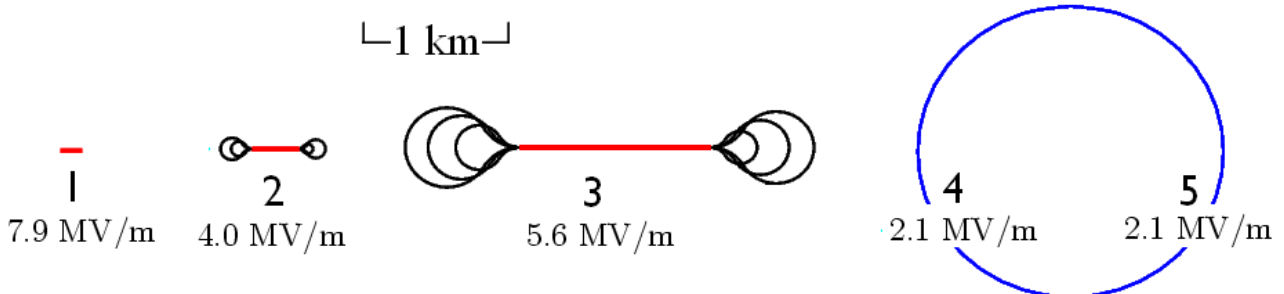


Figure 14: Scale dimensions of second design of acceleration systems without an FFAG. Designed to give improved transmission.

(From param3z2)

	E1 GeV	E2 GeV	Linac m	Lrf m	Larc m	turns	typ	Cav's	Freq MHz	Lcav m	grad MV/m	$\theta$ deg	<grad> MV/m	Decay %	P <sub>peak</sub> MW	t <sub>rf</sub> ms	P <sub>ave</sub> MW	P <sub>wall</sub> MW	N <sub><math>\mu</math></sub> 10 <sup>12</sup>
Linac	0.40	1.5	140	68	0	1.0	SCRF	90	201	0.75	17	18	7.9	2.4	45.7	3.0	2.1	3.4	2.7
RLA	1.5	12.5	306	155	1395	4.4	SCRF	206	201	0.75	17	18	4.0	7.6	104.6	3.0	4.7	7.8	4 × 2.7
RLA	12.5	100	1250	708	7473	6.5	SCRF	1887	402	0.38	20	18	5.6	5.4	469.1	1.0	7.0	11.7	7 × 2.5
RCS	100	400	6283	549	0	23.0	SCRF	2887	805	0.19	25	18	2.1	10.2	395.7	0.5	2.8	4.7	23 × 2.3
RCS	400	750	6283	545	0	27.0	SCRF	2869	805	0.19	25	18	2.1	4.8	393.3	0.7	4.3	7.2	27 × 2.1
	0.40	750.00	14262	2024	8868			7939						27.1	1408		21.0	34.9	2.0

The transmission is now 72.9 %; if we include the early room temperature acceleration the transmission reduces to 63.2 %.

The wall power for rf = 34.8 MW. The Cryostat static losses for a cold length of 140 + 306 + 1395 + 1250 + 7473 = 10.56 km, are estimated as  $12.56 \times 0.9 = 11.3$  MW

The following table gives details of the two dog-bone RLAs. Again, the arcs lengths here are taken from the linear fit to Alex Bogacz's designs shown in fig. 2.

(From paramz2)

	E1 GeV	E2 GeV	dE GeV	L m	slip deg	$\mathcal{E}$ MV/m	Decay %
linac	1.50	2.50	1.00	122.4	40	8.17	0.95
arc	1.50	2.50		209.6		4.77	1.29
linac	2.50	5.00	2.50	306.0	31	8.17	1.32
arc	2.50	5.00		313.9		7.97	0.98
linac	5.00	7.50	2.50	306.0	11	8.17	0.78
arc	5.00	7.50		398.6		6.27	0.84
linac	7.50	10.00	2.50	306.0	5	8.17	0.56
arc	7.50	10.00		472.7		5.29	0.75
linac	10.00	12.50	2.50	306.0	3	8.17	0.43

	E1 GeV	E2 GeV	dE GeV	L m	slip deg	$\mathcal{E}$ MV/m	Decay %
linac	12.50	19.23	6.73	625.0	3	10.77	0.64
arc	12.50	19.23		697.8		9.65	0.58
linac	19.23	32.69	13.46	1250.0	2	10.77	0.79
arc	19.23	32.69		958.1		14.05	0.47
linac	32.69	46.15	13.46	1250.0	1	10.77	0.51
arc	32.69	46.15		1177.6		11.43	0.41
linac	46.15	59.62	13.46	1250.0	0	10.77	0.38
arc	46.15	59.62		1372.7		9.81	0.37
linac	59.62	73.08	13.46	1250.0	0	10.77	0.30
arc	59.62	73.08		1550.7		8.68	0.34
linac	73.08	86.54	13.46	1250.0	0	10.77	0.25
arc	73.08	86.54		1716.0		7.84	0.32
linac	86.54	100.00	13.46	1250.0	0	10.77	0.22

The first RCS in this case, with injection at 100 GeV instead of 30 GeV has a  $6\sigma$  beam height of 10 instead of 18 mm. The ramp rate in the second RCS has been increased from 550 to 707 Hz, which will increase the wall power consumption, now estimated as 3 MW.

### 3.9 Collider Ring for 1.5 TeV c of m

from Y Alexahin [22]

C of m Energy Luminosity	1.5 1	3 4	TeV $10^{34} \text{ cm}^{-2} \text{ sec}^{-1}$
Beam-beam Tune Shift	0.087	0.087	
Muons/bunch	2	2	$10^{12}$
Total Muon Power	7.2	11.5	MW
Ring <bending field>	6	8.4	T
Ring circumference	2.6	4.5	km
$\beta^*$ at IP = $\sigma_z$	10	5	mm
rms momentum spread	0.1	0.1	%
RF frequency	805	805	MHz
RF Voltage	20	230	MV
Repetition Rate	15	12	Hz
Proton Driver power	$\approx 4$	$\approx 4$	MW
Muon Trans Emittance	25	25	pi mm mrad
Muon Long Emittance	72,000	72,000	pi mm mrad

We note that the emittance and bunch intensity requirement same for both examples, making upgrade paths relatively straightforward. The luminosity at 1.5 TeV is somewhat less than CLIC at that energy, but at 3 TeV the luminosity ( $4 \cdot 10^{33}$ ) is a factor of two higher than CLIC's ( $2 \cdot 10^{33}$  for  $dE/E < 1\%$ ), and the muon collider would have two detectors running simultaneously.

RF  $\mathcal{E} = 20$  MV/m super-conducting

$6 \times 18.75 \text{ cm} = 1.12 \text{ m}$  cells for 1.5 TeV  
 $61 \text{ cells} \times 18.75 = 11.4 \text{ m}$  for 3 TeV  
 Static Cryogenic wall power =  $2.6 \times 0.9 = 2.34 \text{ MW}$

### 3.9.1 Ring Magnet Shielding of Decay Electrons

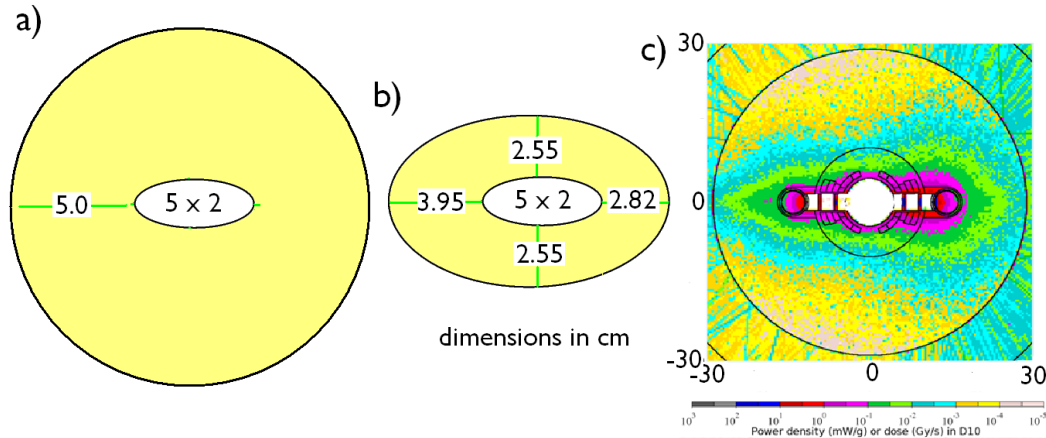


Figure 15: Collider ring magnet shielding options: a) 5 cm thick shielding pipe; b) smaller as asymmetric elliptical pipe; open mid-plane design.

Approximately one third of the total muon beam power (2.5 and 4 MW) is given to decay electrons most of which would, without shielding, end up at 4 K in the ring magnets. For the 1996 Feasibility Study [23], a 5 cm thick tungsten liner (Fig. 15a) was assumed that allowed only 0.27% of this energy to reach the 4 K coils. But this tungsten liner is very large and heavy, and forces the ring magnets to have a very large aperture. With a somewhat larger leakage (1.1% vs. 0.27%) and allowing the shield's shape to reflect the asymmetries of the decay electron distributions is expected to be significantly smaller (fig. 15b). An example of another option using open mid-plane dipoles [24] is shown in Fig. 15c. This design used collimators between magnets, and allowed much smaller aperture magnets, but deposited 4.5% of the energy to be dissipated at 4 K. Other open mid-plane designs are also under study [25].

Assuming a cryogenic efficiency of 20% of the Carnot efficiency (0.27%) the table below gives the wall power needed to cool the three options. For the purposes of the following summary of wall power needs, we will assume option b), not because it is a firm number, but because 10 MW seems a reasonable target, and some method will certainly be able to achieve it.

		1.5 TeV	3 TeV
Beam Power	(MW)	7.2	11.5
Power to decay electrons	MW	2.5	4.0
	leakage %	Wall power MW	Wall power MW
a) 1996 Feasibility Study	0.29	2.6	4.7
b) Elliptical pipe	1.1	10	16.3
c) Open mid-plane	4.5	41	67

## 4 Summaries

### 4.1 Introduction

The following tabulations of 1) muon production and transmissions through the system, and 2) wall power requirements, are meant to give initial approximate estimates. They are based on MARS simulation of pion production and capture, ICOOL simulation of the Neutrino factory phase rotation, the selection of 21 bunches, charge separation at 400 MeV/c in bent solenoids, ICOOL simulations of 6D cooling both before and after the merge, using matrices to generate the required emittance exchange, bunch merging in six dimensions using low frequency rf in the longitudinal phase space and a kicker and trombone system in the transverse dimensions, final cooling in 40 T solenoids with estimates of losses in matching and re-acceleration, followed by analytic estimates of decay losses in acceleration to the energy required in the collider ring.

### 4.2 Production and transmission

	transmission	cumulative	mu/p	mu/pulse
After rotation			0.334	
Momenta = $226 \pm 100$ MeV/c	0.654	1.0	0.219	
Best 21 bunches	0.7	0.7	0.153	$2 \times 27.7 \cdot 10^{12}$
Charge separation	0.85	0.59	0.129	$23.5 \times 2 \cdot 10^{12}$
6D Cooling before merge	0.468	0.28	0.061	$11.0 \times 2 \cdot 10^{12}$
Merge	0.88	0.25	0.055	$9.7 \times 2 \cdot 10^{12}$
6D Cooling after merge	0.48	0.12	0.026	$4.7 \times 2 \cdot 10^{12}$
50 T Cooling	0.7	0.08	0.018	$3.3 \times 2 \cdot 10^{12}$
RTRF low energy acceleration	0.84	0.067	0.015	$2.7 \times 2 \cdot 10^{12}$
SCRF Acceleration	0.73	0.049	0.011	$2.0 \times 2 \cdot 10^{12}$

Note 1: The initial muon production entered here was from the longer Neutrino Factory phase rotation, and the 6D merge used was designed to merge 21 bunches. It is hoped that the newer phase rotation design tabulated above will allow a merge accepting only 12 bunches. That merge will be simpler and probably with higher efficiency than the one in the above table.

Note 2: The numbers of muons given above are those at the end of each specified stage

Note 3: For loading in the 6D cooling before the merge, all bunches are assumed to be transmitted. After the merge, only the selected 21 bunches are assumed.

For  $2 \cdot 10^{12}$  muons, and the above transmission of 0.049, the required initial number of protons per bunch is  $1.87 \cdot 10^{14}$ . This, at 15 Hz and 8 GeV has a power of:

$$15 \times 1.87 \cdot 10^{14} \times 8 \cdot 10^9 \times 1.6 \cdot 10^{-19} = 3.6 \text{ MW}$$

This is less than the 4 MW specified.

### 4.3 Wall Power

#### 4.3.1 Baseline at 1.5 TeV c of m

	Len m	Static 4 K MW	Dynamic rf MW	— PS MW	— 4° MW	— 20° MW	Driver MW	Tot MW
p Driver (SC linac)							20	20
Target and taper	16			11.5	0.4			11.9
Decay and phase rot	95	0.1	0.8		.3			1.2
Charge separation	14							
6D cooling before merge	222	0.6	7.2		6.8	11.4		26
Merge	115	0.2	1.4					1.6
6D cooling after merge	428	0.7	2.8			3.6		7.1
Final 4D cooling	78	0.1	1.5			0.2		1.8
NC RF acceleration	104	0.1	4.1					4.2
SC RF linac	140	0.1	3.4					3.5
SC RF RLAs	10400	9.1	19.5					28.6
SC RF RCSs	12566	11.3	11.8	3.0				26.1
Collider ring	2600	2.3				10		12.4
Totals	26777	24.6	52.5	14.5	17.5	15.1	20	144.3

#### 4.3.2 At 3 TeV instead of 1.5 TeV c of m

- Requires a new RCS for 750-1500 GeV

	E1 GeV	E2 GeV	L m	turns	Cav's	Freq MHz	grad MV/m	<grad> MV/m	Decay %	$P_{wall}$ MW
RCS	750.00	1500.00	12566	29.0	5724	805	25.0	2.1	5.3	15.9

- Requires a larger collider ring
- Wall power changes:

	$\Delta P_{wall}$ MW	$P_{wall}$ total MW	increase %
1.5 TeV		<b>144.3</b>	
rf in new RCS	+15.9	160.2	+11.1
magnet power in RCS	+3	163.3	+1.8
Static cryo in RCS	+11.3	174.5	+6.9
rf in ring	0.15 - 0.1 = +0.14	174.6	+0.07
static cry for larger ring	4.0-2.3=+1.7	176.2	+0.91
Lower rep rate		(12/15 × (176.2 - 37.6) + 37.6) = 148.5	-15.7
More electron leakage	16.3 - 10	154.8	4.2

We see that the wall power for 3 TeV is only 7% higher than at 1.5 TeV.

At 3 TeV, the wall power of 149 MW is  $\approx 1/3$  of the equivalent number (no detector, utilities, etc.) for CLIC; yet it has double the useful (within 1 % E) luminosity (4 vs.  $2 \cdot 10^{34}$ ), and two, instead of one detector. It must be emphasized that these numbers are very preliminary, and probably optimistic. There are large uncertainties and we are not yet claiming that a muon collider is even feasible. Never the less, such numbers certainly motivate continued and more detailed study.

## 5 Conclusion

- Although incomplete and preliminary, we have made a compilation of almost all the rf systems and made a start at a compilation of magnet systems. Many of the parameters given are already out of date, and there are many areas where available parameters have not yet been included. There are certainly many errors.
- These compilations will evolve as corrections are made, more parameters are included, the designs are studied in greater detail, and as choices are made of both parameters and technologies.
- Though not discussed in this document, the greatest technical challenge appears to be the required rf gradients in the specified magnetic fields for the muon cooling. However, the recent achievement[26] of 31 MV/m in 3 T fields, in vacuum at 805 MHz, between beryllium buttons, is encouraging. There has also been recent progress in the study of rf losses in high pressure hydrogen gas.
- Assuming the technical specifications can be achieved, simulations, although far from complete, suggest that the required luminosities are achievable. These luminosities are significantly higher than those for equivalent  $e^+e^-$  linear colliders. For example: at 3 TeV, the muon collider should have a luminosity of  $4 \cdot 10^{33} \text{ cm}^{-2} \text{ s}^{-1}$  and 2 detectors; compared with, for CLIC at energies within 1% of the beam energy, a luminosity of  $2 \cdot 10^{33} \text{ cm}^{-2} \text{ s}^{-1}$  and one detector at a time.
- Assuming the technical specifications can be achieved, the wall power consumption of muon colliders appears to be significantly less than for equivalent linear collider designs. For example: at 3 TeV, the muon collider should use less than 200 MW, compared with over 400 MW for CLIC.
- The fundamental reason for the lower power consumption per luminosity, is that the muons collide hundreds of times, while the electron bunches can collide only once. This allows significantly less beam power. e.g. 11.5 MW instead of 28 MW for the 3 TeV CLIC. In addition, since the muons can be accelerated in rings with many turns, higher efficiencies should be possible. Another reason for the higher luminosities is the suppression of beamstrahlung by the higher muon mass, allowing all interactions to occur at the full beam energies.

## Acknowledgement

The author thanks R. Fernow and J.C. Gallardo for their help in finishing this manuscript.

## References

- [1] The IDS-NF Collaboration, Interim Design Report, IDS-NF-020, 19 March 2011.
- [2] R. Palmer et al, Scheme for ionization cooling for a muon collider, PoS (Nufact08) 019, 2008.
- [3] R. Palmer & R. Fernow, Tapered six-dimensional cooling channel for a muon collider, Proc. PAC11, New York, p. 106.
- [4] K. Yonehara et al, A helical cooling channel system for muon colliders, Proc. IPAC'10, Kyoto, Japan, p. 870.
- [5] Y. Alexahin, Circularly inclined solenoid channel for 6D ionization cooling of muons, Proc. PAC09, Vancouver, CA, p. 727.
- [6] A. Bogacz, Muon RLA - design status and new options, talk at MAP Winter Meeting, JLAB, February 28-March 4, 2011.

- [7] D. Summers et al, Muon acceleration to 750 GeV in the Tevatron tunnel for a 1.5 muon collider, Proc. PAC07, Albuquerque, NM, p. 3178.
- [8] The MICE Collaboration, An International Ionization Cooling Experiment, submitted to Rutherford Appleton Laboratory, 10 January 2003.
- [9] Compare Feasibility Study II (op. cit.), p. 11-9.
- [10] Feasibility Study II of a Muon-based Neutrino Source, S. Ozaki, R. Palmer, M. Zisman & J. Gallardo (eds), BNL-52623, 2001.
- [11] K. Gollwitzer, Task force on Project X for muon collider, talk at Muon Collider 2011 Workshop, Telluride, CO, June 27-July 1, 2011.
- [12] G. Flanagan et al, Using Project X as a proton driver for muon colliders and neutrino factories, Proc. IPAC'10, Kyoto, Japan, p. 4452.
- [13] N. Souchlas et al, Beam-power deposition in a 4-MW target station for a muon collider or a muon collider, Proc. IPAC'10, Kyoto, Japan.
- [14] D. Neuffer et al, Muon capture in the front end of the IDS neutrino factory, Proc. IPAC'10, Kyoto, Japan, p. 3500.
- [15] D. Neuffer & C. Yoshikawa, Muon capture for the front end of a  $\mu^+\mu^-$  Collider, Proc. PAC11, New York, p. 157.
- [16] R. Palmer & R. Fernow, Charge separation for muon collider cooling, Proc. PAC11, New York, p. 103.
- [17] R. Palmer et al, A complete scheme for a muon collider, Proc. COOL 2007, Bad Kreuznach, Germany, p. 77.
- [18] C. Yoshikawa et al, Bunch coalescing in a helical channel, unpublished report NFMCC-doc-566, 28 July 2011.
- [19] R. Palmer & R. Fernow, Six-dimensional bunch merging for muon collider cooling, Proc. PAC11, New York, p. 109.
- [20] C. Yoshikawa, private communication.
- [21] R. Palmer et al, Muon collider final cooling in 30-50 T solenoids, Proc. PAC11, New York, p. 2061.
- [22] Y. Alexahin et al, Conceptual design of the muon collider ring lattice, Proc. IPAC'10, Kyoto, Japan, p. 1563.
- [23]  $\mu^+\mu^-$  Collider - A Feasibility Study, BNL-52503, Fermi Lab-Conf-96/092, LBNL-38946
- [24] N. Mokhov et al, Magnet Designs for Muon Collider Ring and Interaction Regions, <http://accelconf.web.cern.ch/AccelConf/IPAC10/papers/mopeb053.pdf>
- [25] R.J. Weggel et al, Open Midplane Dipoles for a Muon Collider, <http://accelconf.web.cern.ch/AccelConf/PAC2011/papers/tup177.pdf>; P. McIntyre, Open-midplane Dipole and Decay Electron Dynamics in MR Ring Dipoles, <https://indico.fnal.gov/conferenceDisplay.py?confId=4404>
- [26] A. Moretti, <https://indico.fnal.gov/conferenceDisplay.py?confId=5049>.